A Regulatory Module Controlling Homeostasis of a Plant Immune Kinase

Wang, Jinlong ; Grubb, Lauren E ; Wang, Jiayu ; Liang, Xiangxiu ; Li, Lin ; Gao, Chulei ; Ma, Miaomiao ; Feng, Feng ; Li, Meng ; Li, Lei ; Zhang, Xiaojuan ; Yu, Feifei ; Xie, Qi ; Chen, She ; Zipfel, Cyril ; Monaghan, Jacqueline ; Zhou, Jian-Min

DOI: https://doi.org/10.1016/j.molcel.2017.12.026

Article

Molecular Cell

A Regulatory Module Controlling Homeostasis of a Plant Immune Kinase

Graphical Abstract

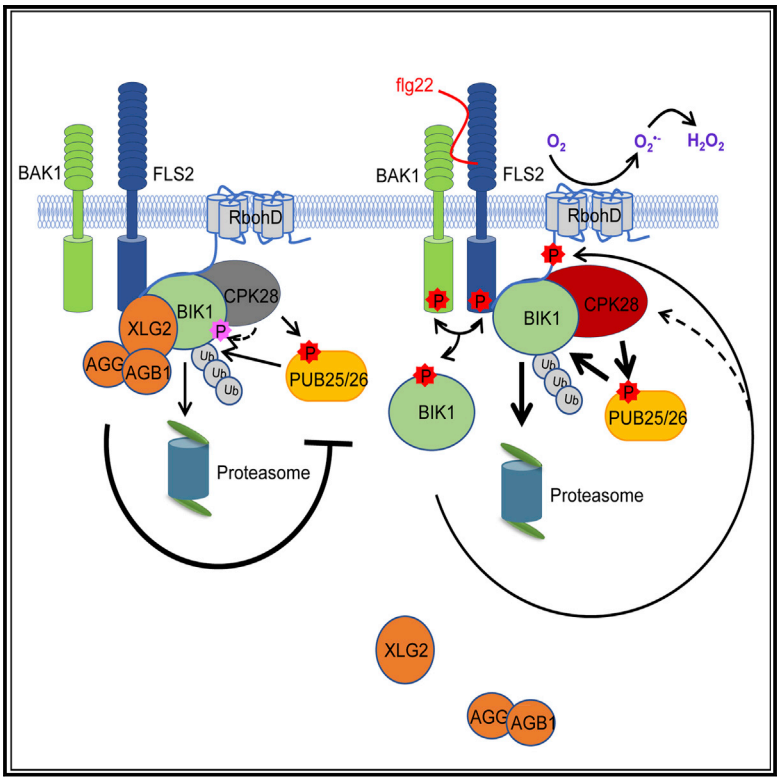

Authors

Jinlong Wang, Lauren E. Grubb, Jiayu Wang, ..., Cyril Zipfel, Jacqueline Monaghan, Jian-Min Zhou

Correspondence

jmzhou@genetics.ac.cn

In Brief

Dynamic control of the stability of the key immune regulatory kinase BIK1 is critical for proper immune function in plants. The authors identified a pair of BIK1-targeting E3 ligases, PUB25 and PUB26, that form a regulatory module with the calcium-dependent protein kinase CPK28 and heterotrimeric G proteins to promote or inhibit BIK1 degradation, thereby maintaining homeostasis of BIK1 and immunity.

Highlights

- The E3 ligases PUB25/26 target non-activated immune kinase BIK1 for degradation
- PUB25/26 negatively regulate immune responses and disease resistance
- CPK28 phosphorylates PUB25/26 to enhance their E3 activity and BIK1 degradation
- Heterotrimeric G proteins directly inhibit PUB25/26 E3 activity to stabilize BIK1

Wang et al., 2018, Molecular Cell 69, 493–504
February 1, 2018
https://doi.org/10.1016/j.molcel.2017.12.026

CellPress

Molecular Cell
Article

A Regulatory Module Controlling Homeostasis of a Plant Immune Kinase

Jinlong Wang,[1,5] Lauren E. Grubb,[2] Jiayu Wang,[1] Xiangxiu Liang,[1] Lin Li,[3] Chulei Gao,[1] Miaomiao Ma,[1] Feng Feng,[1] Meng Li,[1] Lei Li,[1] Xiaojuan Zhang,[1] Feifei Yu,[1] Qi Xie,[1] She Chen,[3] Cyril Zipfel,[4] Jacqueline Monaghan,[2] and Jian-Min Zhou[1,5,6,*]

[1]State Key Laboratory of Plant Genomics, Institute of Genetics and Developmental Biology, Chinese Academy of Sciences, No.1 West Beichen Road, Chaoyang District, Beijing 100101, China
[2]Biology Department, Queen's University, Kingston, ON K7L 3N6, Canada
[3]National Institute of Biological Sciences, Beijing, No. 7 Science Park Road ZGC Life Science Park, Beijing 102206, China
[4]Sainsbury Laboratory, Norwich Research Park, Norwich NR4 7UH, UK
[5]University of Chinese Academy of Sciences, No. 19 (A) Yuquan Road, Shijingshan District, Beijing 100049, China
[6]Lead Contact
*Correspondence: jmzhou@genetics.ac.cn
https://doi.org/10.1016/j.molcel.2017.12.026

SUMMARY

Plant pattern recognition receptors (PRRs) perceive microbial and endogenous molecular patterns to activate immune signaling. The cytoplasmic kinase BIK1 acts downstream of multiple PRRs as a rate-limiting component, whose phosphorylation and accumulation are central to immune signal propagation. Previous work identified the calcium-dependent protein kinase CPK28 and heterotrimeric G proteins as negative and positive regulators of BIK1 accumulation, respectively. However, mechanisms underlying this regulation remain unknown. Here we show that the plant U-box proteins PUB25 and PUB26 are homologous E3 ligases that mark BIK1 for degradation to negatively regulate immunity. We demonstrate that the heterotrimeric G proteins inhibit PUB25/26 activity to stabilize BIK1, whereas CPK28 specifically phosphorylates conserved residues in PUB25/26 to enhance their activity and promote BIK1 degradation. Interestingly, PUB25/26 specifically target non-activated BIK1, suggesting that activated BIK1 is maintained for immune signaling. Our findings reveal a multi-protein regulatory module that enables robust yet tightly regulated immune responses.

INTRODUCTION

Plasma membrane-localized plant pattern recognition receptors (PRRs) such as FLS2, EFR, PEPRs, and LYK5 detect a variety of endogenous and microbial molecular patterns generated during pathogen attacks and trigger powerful defenses (Tang et al., 2017; Zipfel and Oldroyd, 2017). These PRRs and their co-receptors, such as BAK1 and CERK1, directly interact with and activate downstream immune signaling through a class of related receptor-like cytoplasmic kinases (RLCKs) that includes BIK1 and related PBS1-like (PBL) proteins (Lu et al., 2010; Zhang et al., 2010). BIK1 and PBLs are of central importance to the plant immune system as they regulate key signaling events, including transient bursts of calcium and reactive oxygen species (ROS) (Kadota et al., 2014; Li et al., 2014; Monaghan et al., 2015; Ranf et al., 2014), increased synthesis of salicylic acid (Kong et al., 2016), and activation of mitogen-activated protein kinases (Yamada et al., 2016). Multiple pathogen virulence effectors target BIK1 and PBLs to inhibit plant immunity (Feng et al., 2012; Liu et al., 2011; Zhang et al., 2010), further highlighting the importance of this family of kinases in plant immunity.

Recent work has demonstrated the importance of BIK1 regulation in immune homeostasis. First, BIK1 phosphorylation, which is prerequisite for BIK1 activation, is subject to negative regulation by the protein phosphatase PP2C38 (Couto et al., 2016). Second, BIK1 stability is positively regulated by heterotrimeric G proteins composed of XLG2/XLG3 (Gα), AGB1 (Gβ), and AGG1/AGG2 (Gγ) and negatively regulated by the calcium-dependent protein kinase CPK28 through the ubiquitin proteasome system (Liang et al., 2016; Monaghan et al., 2014). However, the identity of the E3 ubiquitin ligase(s) that target BIK1 and the detailed regulatory mechanisms that control its stability remain elusive.

Here we report the identification of two phylogenetically related plant U-box domain-containing proteins, PUB25 and PUB26, as E3 ligases that target BIK1 for degradation and negatively regulate BIK1-mediated immunity. Both CPK28 and the heterotrimeric G proteins exert their regulations on BIK1 stability through PUB25/26. Whereas CPK28 phosphorylates PUB25/26 to enhance E3 ligase activity and BIK1 degradation, the heterotrimeric G proteins directly inhibit PUB25/26 E3 ligase activity to stabilize BIK1. We additionally found that PUB25/26 specifically ubiquitinate non-activated BIK1, which is expected to indirectly limit the size of activated BIK1 pool. We propose a model in which PUB25/26, the G proteins, and CPK28 form a signaling module that regulates not only the total amount, but also the proportion of activated BIK1 protein before and after immune activation, thereby controlling immune homeostasis.

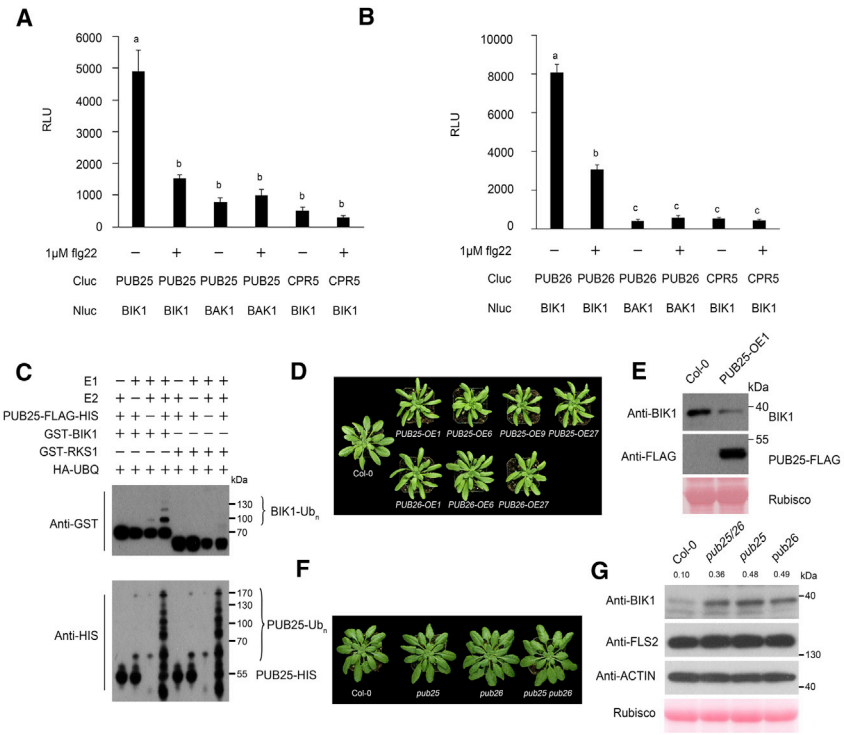

Figure 1. PUB25/26 Interact with and Ubiquitinate BIK1

(A and B) BIK1 interacts with PUB25/26 *in planta*. Split-luciferase assays were conducted with the indicated constructs in the presence or absence of 1 μM flg22. BAK1-HA-Nluc and Cluc-CPR5 were used as negative controls. Values represent mean relative luminescence units (RLU) ± SDs (n = 8). Different letters indicate significant difference at $p < 0.05$.

(C) PUB25 ubiquitinates BIK1. *In vitro* ubiquitination assays were carried out with the indicated recombinant proteins, and ubiquitination of GST-BIK1/RKS1 and PUB25-FLAG-HIS was detected by immunoblot using anti-GST and anti-HIS antibodies, respectively.

(D) Rosette morphology of independent *PUB25/26*-overexpression (OE) lines 5 weeks after germination grown in short-day conditions.

(E) Overexpression of *PUB25-FLAG* reduces BIK1 abundance in plants. Col-0 and the *PUB25-OE1* line were examined by immunoblot using anti-BIK1 antibodies. Anti-FLAG immunoblot confirmed the presence of PUB25-FLAG, and Ponceau S staining of Rubisco confirmed equal loading.

(F) Rosette morphology of *pub25*, *pub26*, and *pub25 pub26* (*pub25/26*) double mutant plants alongside Col-0 at 5 weeks post-germination grown in short-day conditions.

(G) Mutations in *PUB25/26* increase BIK1 stability in plants. BIK1 levels in plants of the indicated genotypes were detected by immunoblot using anti-BIK1 antibodies. Accumulation of FLS2 and ACTIN was detected using anti-FLS2 and anti-ACTIN antibodies. Ponceau S staining of Rubisco is included as a loading control. Numbers indicate arbitrary units of BIK1 calculated from densitometry measurements normalized to total Rubisco protein.

The experiments were repeated at least twice (A and B) or three times (C, E, and G) with similar results.

See also Figure S1 and Table S1.

RESULTS

PUB25/26 Are Ubiquitin E3 Ligases that Promote BIK1 Degradation

In an effort to identify BIK1-interacting proteins, we transiently expressed BIK1-FLAG in *Arabidopsis* protoplasts, immunoprecipitated BIK1-FLAG, and analyzed the immunoprecipitated product composition by liquid chromatography-tandem mass spectrometry (LC-MS/MS). One candidate protein identified in two independent experiments, but absent in controls lacking a FLAG-tagged protein, was the U-box domain-containing protein PUB25 (Table S1). Split-luciferase complementation assays in *Nicotiana benthamiana* confirmed that PUB25 specifically interacted with BIK1, but not BAK1 (Figure 1A). Co-immunoprecipitation (coIP) in *Arabidopsis* protoplasts further confirmed this association (Figure S1A). A close homolog of PUB25, PUB26, similarly interacted with BIK1 (Figures 1B and S1B). Treatment of *N. benthamiana* plants or *Arabidopsis* protoplasts with flg22 greatly reduced the interaction, suggesting ligand-induced dissociation between the protein pairs. Flg22 treatment induces BIK1 phosphorylation and slower migration in SDS-PAGE (Figure S1A; Lu et al., 2010; Zhang et al., 2010). This phosphorylated BIK1 is referred to as hyper-phosphorylated, whereas the fast-migrating BIK1 before flg22 treatment is referred to as under-phosphorylated in the following text. Interestingly, the flg22-induced dissociation was not detected when a kinase-dead $BIK1^{K105E}$-HA mutant protein was used (Figures S1A and S1B). Unlike wild-type BIK1, $BIK1^{K105E}$ does not undergo hyper-phosphorylation when plants or protoplasts are treated with flg22 (Zhang et al., 2010), suggesting that the kinase activity or hyper-phosphorylation of BIK1 is required for flg22-induced dissociation. Only the under-phosphorylated BIK1 (Zhang et al., 2010) co-precipitated with PUB25/26, whereas the hyper-phosphorylated form did not (Figures S1A–S1C). These data suggest that PUB25/26 primarily interact with the under-phosphorylated form of BIK1.

FLS2 is known to associate with additional RLCKs for signaling, including PBL1 and BSK1 (Shi et al., 2013; Zhang et al., 2010). CoIP assays in protoplasts showed that PUB25/26 can also associate with PBL1 and BSK1, and that the associations diminished upon flg22 treatment (Figures S1D and S1E), indicating that PUB25/26 may target multiple RLCKs associated with FLS2.

In vitro ubiquitination assays (Zhao et al., 2012) were performed to determine whether BIK1 is a substrate of PUB25/26. Incubation of recombinant GST-BIK1 with recombinant PUB25-FLAG-HIS, HA-ubiquitin (HA-UBQ), a His-tagged E2 ubiquitin-conjugating enzyme, and a His-tagged E1 ubiquitin-activating enzyme led to production of laddering bands only in the presence of E1, E2, and PUB25 (Figure 1C), indicating

poly-ubiquitination of GST-BIK1. In contrast, GST-tagged RKS1, an RLCK not involved in FLS2 signaling (Wang et al., 2015), was not ubiquitinated. PUB25-FLAG-HIS was auto-ubiquitinated in both reactions. These data indicate that PUB25 is an E3 ubiquitin ligase and can ubiquitinate BIK1 *in vitro*.

To determine whether PUB25/26 can promote BIK1 degradation *in planta*, we co-expressed PUB25/26-FLAG with BIK1-HA in *Arabidopsis* protoplasts and examined BIK1-HA protein levels in the presence of cycloheximide (CHX), which inhibits *de novo* protein synthesis. Overexpression of PUB25/26-FLAG significantly reduced BIK1-HA abundance (Figure S1F), suggesting that PUB25/26 can promote BIK1 degradation. The abundance of kinase-dead BIK1^{K105E}-HA was similarly reduced when co-expressed with PUB25/26 (Figure S1F). Treatment of protoplasts with the proteasome inhibitor MG132 restored BIK1-HA to a level comparable to protoplasts expressing BIK1-HA alone, which is consistent with PUB25/26 promoting BIK1 degradation through the proteasome system.

To further test whether PUB25/26 regulate BIK1 stability in plants, we generated multiple transgenic lines overexpressing either *PUB25* or *PUB26* (*PUB25/26*-OE). All lines accumulated *PUB25/26* transcripts to high levels (Figure S1G) and developed a distinctive swirling rosette phenotype (Figure 1D), reminiscent of hyperactive brassinosteroid (BR) signaling caused by overexpression of *BRI1* or the BR-biosynthetic gene *DWF4* (Choe et al., 2001; Wang et al., 2001). As BIK1 is known to negatively regulate BR signaling (Lin et al., 2013), the phenotype is consistent with a negative regulation of BIK1 stability. To facilitate detection of the BIK1 protein, we raised antibodies that specifically detected BIK1 in Col-0, but not *bik1* plants (Figure S1H). The BIK1 protein level (Figure 1E), but not *BIK1* transcripts (Figure S1I), was greatly diminished in the *PUB25-OE1* line compared to Col-0 plants, indicating that *PUB25* overexpression reduced BIK1 level in a post-transcriptional manner. To further determine the role of PUB25/26 in BIK1 accumulation in plants, we isolated null *pub25* and *pub26* T-DNA insertional mutants and constructed a *pub25 pub26* double mutant (Figures S1J and S1K). All mutants were morphologically similar to Col-0 (Figure 1F). While the *BIK1* transcript level was not affected in the *pub25 pub26* double mutant (Figure S1L), BIK1 protein accumulated to higher levels in *pub25*, *pub26*, and *pub25 pub26* mutants compared to Col-0 (Figure 1G). In contrast, all plants accumulated similar amounts of FLS2, indicating that PUB25/26 specifically control BIK1 stability, at least in the context of the FLS2 immune complex. It is interesting to note that the *pub25 pub26* double mutant did not show more BIK1 accumulation than did *pub25* and *pub26* single mutants, suggesting that both PUB25 and PUB26 are required to regulate BIK1 stability.

PUB25/26 Negatively Regulate BIK1-Mediated Immunity

We next tested whether PUB25/26 play a role in pattern-triggered immune response. The flg22-induced ROS burst was significantly elevated in *pub25* and *pub26* single mutants (Figures S2A and S2B), as well as the *pub25 pub26* double mutant compared to Col-0 (Figure 2A). We further inoculated these plants with the fungal pathogen *Botrytis cinerea* and the non-virulent bacterial strain *Pseudomonas syringae* pv. *tomato* (*Pto*) DC3000 *hrcC*$^{-}$ to test whether PUB25/26 play a role in regulating disease resistance. We used the *Pto* DC3000 *hrcC*$^{-}$ strain instead of the wild-type strain because the latter secretes a variety of effectors to suppress pattern-triggered immunity, which can obscure the analysis of this signaling pathway (Feng and Zhou, 2012; Macho and Zipfel, 2015). Compared to Col-0, *pub25*, *pub26*, and *pub25 pub26* mutants showed smaller lesions when inoculated with *B. cinerea* (Figure 2B) and reduced bacterial populations when inoculated with *Pto* DC3000 *hrcC*$^{-}$ (Figure 2C). Because the *pub25 pub26* double mutant largely resembles *pub25* and *pub26* single mutants, these analyses suggest that both PUB25 and PUB26 function in *Arabidopsis* immunity. Comparatively, *PUB25-OE* lines were severely diminished in flg22-triggered ROS burst (Figure 2D) and exhibited increased susceptibility to both *B. cinerea* (Figure 2E) and *Pto* DC3000 *hrcC*$^{-}$ (Figure 2F). These results demonstrate a negative role of PUB25/26 in flg22-induced immune responses and disease resistance to both fungal and bacterial pathogens. To determine whether the diminished BIK1 accumulation accounts for the impaired immunity in *PUB25-OE* plants, we introduced a *BIK1-HA* transgene under the control of its native promoter (*NP::BIK1-HA*; Zhang et al., 2010) into the *PUB25-OE1* line by crossing, which is known to increase BIK1 level in the recipient line. As previously reported (Liang et al., 2016; Monaghan et al., 2014), expression of the *NP::BIK1-HA* transgene increased flg22-triggered ROS burst (Figure 2G). While the *PUB25-OE1* line was severely impaired in flg22-triggered ROS burst, introduction of the *NP::BIK1-HA* transgene restored ROS production to wild-type levels (Figure 2G), indicating that the impaired immune response in the *PUB25-OE* line was indeed caused by the diminished BIK1 accumulation. Consistent with this result, the *NP::BIK1-HA* transgene also reduced *B. cinerea* susceptibility in the *PUB25-OE* line (Figure 2H). Taken together, these findings demonstrate that PUB25/26 negatively regulate flg22-triggered immune response and disease resistance, likely through controlling BIK1 stability.

PUB25/26 Specifically Poly-ubiquitinate Non-activated BIK1

The differential interactions between PUB25/26 with hyper- or under-phosphorylated BIK1 (Figures S1A and S1B) prompted us to test whether these PUBs selectively target under-phosphorylated BIK1 for degradation. Indeed, whereas overexpression of *PUB25/26* greatly destabilized BIK1 in CHX-treated protoplasts, it had a mild effect when the protoplasts were additionally treated with flg22 (Figures 3A and 3B). In contrast, the BIK1^{K105E} mutant protein, which does not undergo flg22-induced hyper-phosphorylation, was not stabilized upon flg22 treatment (Figure 3B). BIK1 is known to be phosphorylated at multiple sites following flg22 perception, including Ser236 and Thr237, which are located in the activation loop and are highly conserved in BIK1 and PBLs and necessary for kinase activation (Lu et al., 2010; Zhang et al., 2010). We generated phospho-dead BIK1$^{S236A/T237A}$ (BIK1^{2A}) and phospho-mimetic BIK1$^{S236D/T237D}$ (BIK1^{2D}) variants to determine whether the phosphorylation of these sites affects PUB25/26-BIK1 association and subsequent degradation. We measured the stability of these BIK1 variants co-expressed with PUB25 in the presence of CHX. Similar to

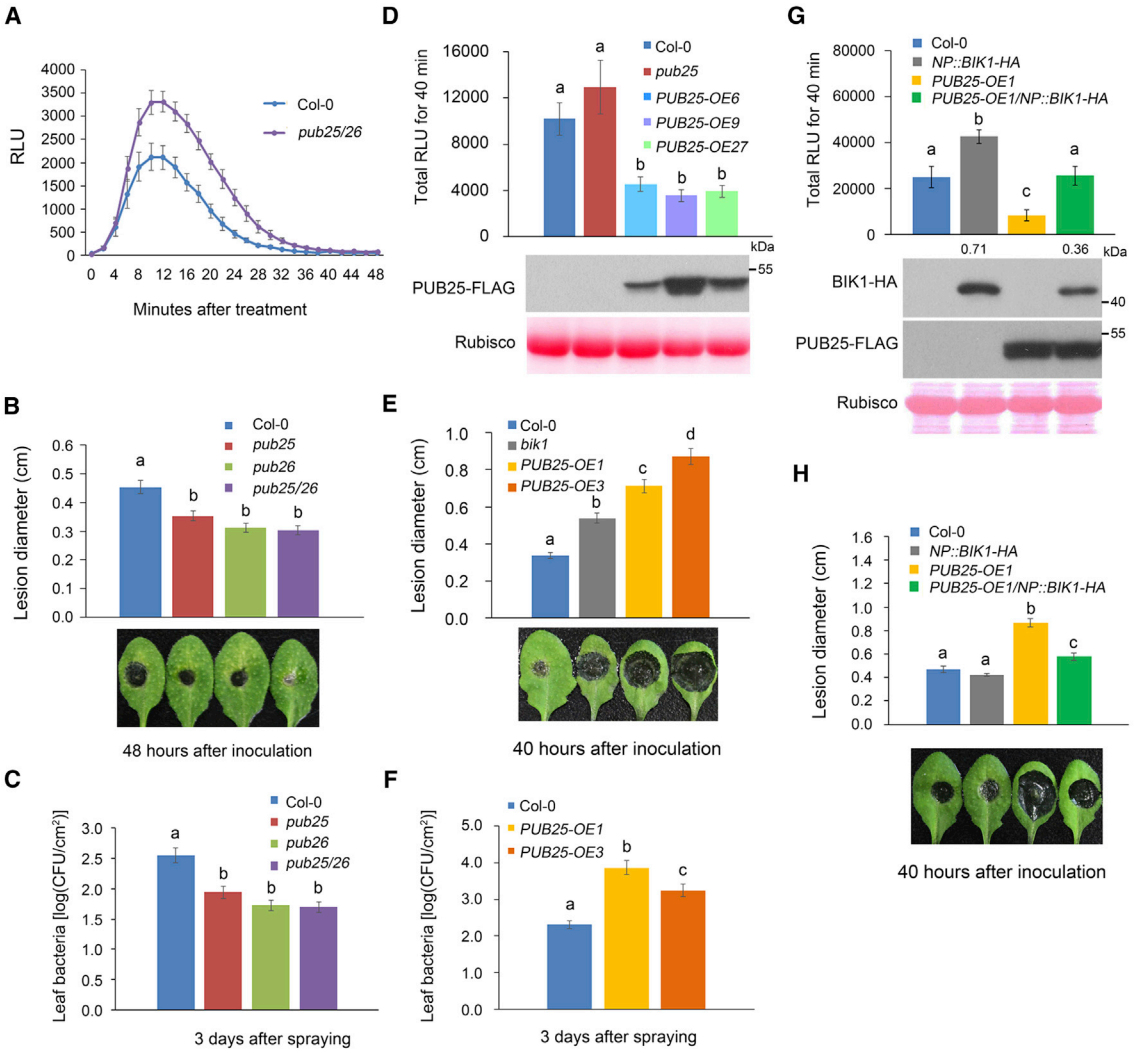

Figure 2. PUB25/26 Negatively Regulate Plant Immunity by Controlling BIK1 Levels

(A–C) *pub25*, *pub26*, and *pub25/26* mutants display enhanced ROS burst in response to flg22 (A), increased disease resistance to *B. cinerea* (B), and elevated resistance to *Pto* DC3000 *hrcC*$^{-}$ (C).

(D–F) *PUB25-OE* lines are compromised in flg22-induced ROS burst (D), disease resistance to *B. cinerea* (E), and resistance to *Pto DC3000 hrcC*$^{-}$ (F).

(G and H) Introduction of the *NP::BIK1-HA* transgene into the *PUB25-OE1* line restores flg22-induced ROS production (G) and disease resistance to *B. cinerea* (H). Note that the accumulation of BIK1-HA is reduced in the presence of *PUB25-OE1* background (G).

For ROS burst (A, D, and G), leaves of the indicated genotypes were induced with 1 μM flg22, and relative amounts of H_2O_2 (expressed as RLU; relative luminescence units) were measured immediately. Values are means ± SDs (n = 8).

For disease resistance to *B. cinerea* (B, E, and H), leaves of the indicated genotype were inoculated with *B. cinerea*, and lesion size was measured at the indicated time. Values are means ± SDs (n > 12). Photographs of representative infected leaves are shown under the histogram.

For resistance to *Pto DC3000 hrcC*$^{-}$ (C and F), plants were spray-inoculated and bacterial growth was assessed 3 days later. Values are means of colony-forming units per leaf area (CFU/cm^2) ± SDs (n = 12).

Different letters indicate significant differences at $p < 0.05$. Each experiment was repeated three times with similar results. *pub25* and *pub26* refer to *pub25-1* and *pub26-1*, respectively.

See also Figure S2.

wild-type BIK1, BIK1^{2A} was destabilized by *PUB25* overexpression in protoplasts, whereas BIK1^{2D} was largely stable (Figure 3C), supporting the idea that PUB25 is unable to destabilize BIK1 when S236/T237 are phosphorylated. CoIP assays showed that BIK1, BIK1^{2A}, and BIK1^{2D} similarly associated with PUB25 in protoplasts (Figures S3A–S3C), indicating that phosphorylation at these sites did not affect BIK1 association with PUB25/26. The results indicate that the insensitivity of BIK1^{2D} to PUB25/26-mediated degradation was not simply due to lack of association and suggest that other phosphosites may be responsible for flg22-induced dissociation. We therefore tested whether the phosphorylation of BIK1$^{S236/T237}$ impacts PUB25-mediated

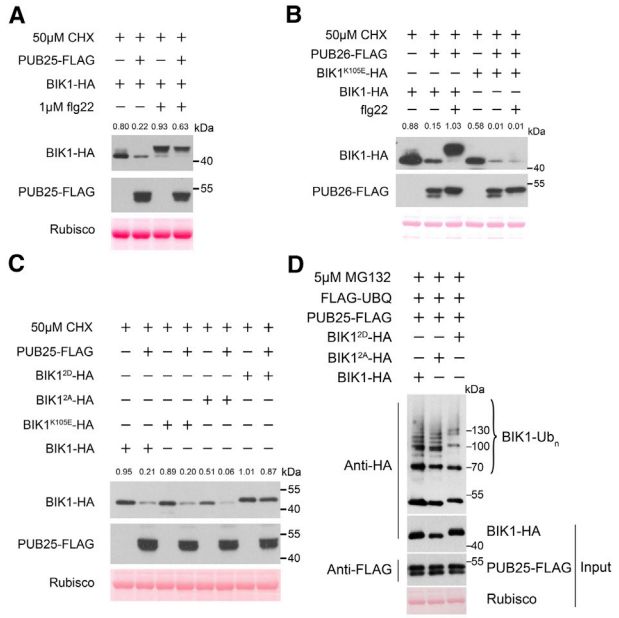

Figure 3. PUB25/26 Specifically Mark Non-activated BIK1 for Degradation

(A and B) Flg22 treatment stabilizes BIK1-HA in *Arabidopsis* protoplasts overexpressing *PUB25-FLAG* (A) and *PUB26-FLAG* (B). Protoplasts expressing the indicated proteins were treated with 50 μM CHX and 1 μM flg22 for 2 hr before total protein was examined with immunoblot. Ponceau S indicates equal loading. Numbers indicate arbitrary units of BIK1-HA calculated from densitometry measurements normalized to total Rubisco protein.

(C) PUB25 destabilizes wild-type and phospho-dead forms BIK1, but not a phospho-mimetic variant. Col-0 protoplasts co-expressing PUB25-FLAG with wild-type BIK1-HA, $BIK1^{2A}$-HA ($BIK1^{S236A/T237A}$), or $BIK1^{2D}$-HA ($BIK1^{S236D/T237D}$) were treated with 50 μM CHX for 2 hr before immunoblot analysis.

(D) $BIK1^{2D}$ showed much less PUB25-induced poly-ubiquitination compared to BIK1 and $BIK1^{2A}$ in protoplasts. Col-0 protoplasts transfected with FLAG-UBQ, PUB25-FLAG, and BIK1-HA variants were incubated overnight in the presence of 5 μM MG132. Ubiquitinated BIK1-HA was isolated with anti-FLAG beads, and BIK1 ubiquitination was detected with an anti-HA antibody.

Numbers indicate arbitrary units of BIK1 calculated from densitometry measurements normalized to total Rubisco protein (A–C).

Each experiment was repeated three times with similar results.

See also Figure S3.

poly-ubiquitination by co-expressing wild-type or mutant forms of BIK1-HA with PUB25-FLAG and FLAG-UBQ in protoplasts. Anti-HA immunoblot detected strong laddering bands indicative of poly-ubiquitination of BIK1-HA and $BIK1^{2A}$-HA proteins, whereas $BIK1^{2D}$-HA was much less poly-ubiquitinated (Figure 3D). Together, these results suggest that PUB25/26 associate with BIK1 irrespective of the S236/T237 phosphorylation status, but selectively mark under-phosphorylated BIK1 for ubiquitination and degradation.

CPK28 Acts Together with PUB25/26 to Regulate BIK1 Stability and Immune Responses

The ability of PUB25/26 to negatively regulate BIK1 and immunity is reminiscent of CPK28 (Monaghan et al., 2014), suggesting that they act in the same pathway. Split-luciferase and coIP assays showed that CPK28 associated with PUB25/26 regardless of flg22 treatment (Figures 4A, 4B, and S4A), suggesting that CPK28 and PUB25/26 act together to control BIK1 stability. A *pub25 pub26 cpk28* triple mutant was generated to further test this possibility. Immunoblot analyses showed that endogenous BIK1 accumulated to a high level in *cpk28* compared to Col-0 (Figure 4C), which is consistent with the previous report (Monaghan et al., 2014). BIK1 accumulation was also increased in *pub25 pub26* plants, although slightly less than that in *cpk28*, and the *pub25 pub26 cpk28* triple mutant showed similar BIK1 levels compared to *cpk28* (Figure 4C). Consistent with this, *cpk28* and *pub25 pub26 cpk28* were similarly enhanced in flg22-induced ROS production (Figure 4D). The lack of an additive effect in the triple mutant supports the possibility that they act in the same pathway to promote BIK1 degradation. We reasoned that PUB25/26, as E3 ligases, may function downstream of CPK28 to regulate BIK1 stability. We therefore tested whether *PUB25* overexpression could reduce the flg22-triggered ROS burst in the *cpk28* mutant. Indeed, introgression of the *PUB25-OE1* transgene into *cpk28* by crossing significantly reduced flg22-induced ROS production in these plants (Figure 4E). These data support the idea that PUB25/26 act downstream of CPK28 to buffer flg22-triggered immune signaling. Given that *cpk28* accumulated an even higher level of BIK1 and showed much greater flg22-induced ROS burst than did *pub25 pub26* double mutant (Figures 4C and 4D), additional PUBs may also control BIK1 stability downstream of CPK28. In *Arabidopsis*, three additional PUBs, PUB22, PUB23, and PUB24, are related to PUB25/26 in sequence and have been shown to negatively regulate pattern-triggered immunity (Trujillo et al., 2008). Co-expressing PUB22/23 strongly destabilized BIK1 in protoplasts (Figures S4B and S4C), suggesting that these E3 ligases also play a role in BIK1 degradation.

CPK28 can phosphorylate BIK1 *in vitro*, although the phosphorylation sites remain to be determined (Monaghan et al., 2014). In the absence of flg22 perception, CPK28 negatively regulates BIK1 stability. We first sought to determine whether BIK1 S236/T237 contribute to overall phosphorylation by CPK28 *in vitro*. Incubation with CPK28 resulted in phosphorylation of recombinant $BIK1^{K105E}$ protein (Figure S4D). Introduction of S236A/T237A mutations into $BIK1^{K105E}$ ($BIK1^{K105E/2A}$) did not impact overall phosphorylation by CPK28, indicating that S236/T237 are not major phosphosites for CPK28. CoIP assays showed that the BIK1-CPK28 interaction was not affected by $BIK1^{2A}$ and $BIK1^{2D}$ mutations (Figure S4E), further suggesting that S236/T237 do not impact the regulation of BIK1 by CPK28. Furthermore, the BIK1-PUB25 interaction occurred similarly in *cpk28* mutant and CPK28-OE protoplasts (Figure S4F). Overall, these findings are consistent with previous findings that S236/T237 are phosphorylated by BAK1 upon flg22 perception (Lu et al., 2010; Feng et al., 2012), and that CPK28 does not affect BIK1-PUB25 interaction.

CPK28 Phosphorylates PUB25/26 to Enhance E3 Ligase Activity and BIK1 Degradation

Throughout our work, we found that PUB25/26-FLAG existed in slow- and fast-migrating forms, and that treatment with

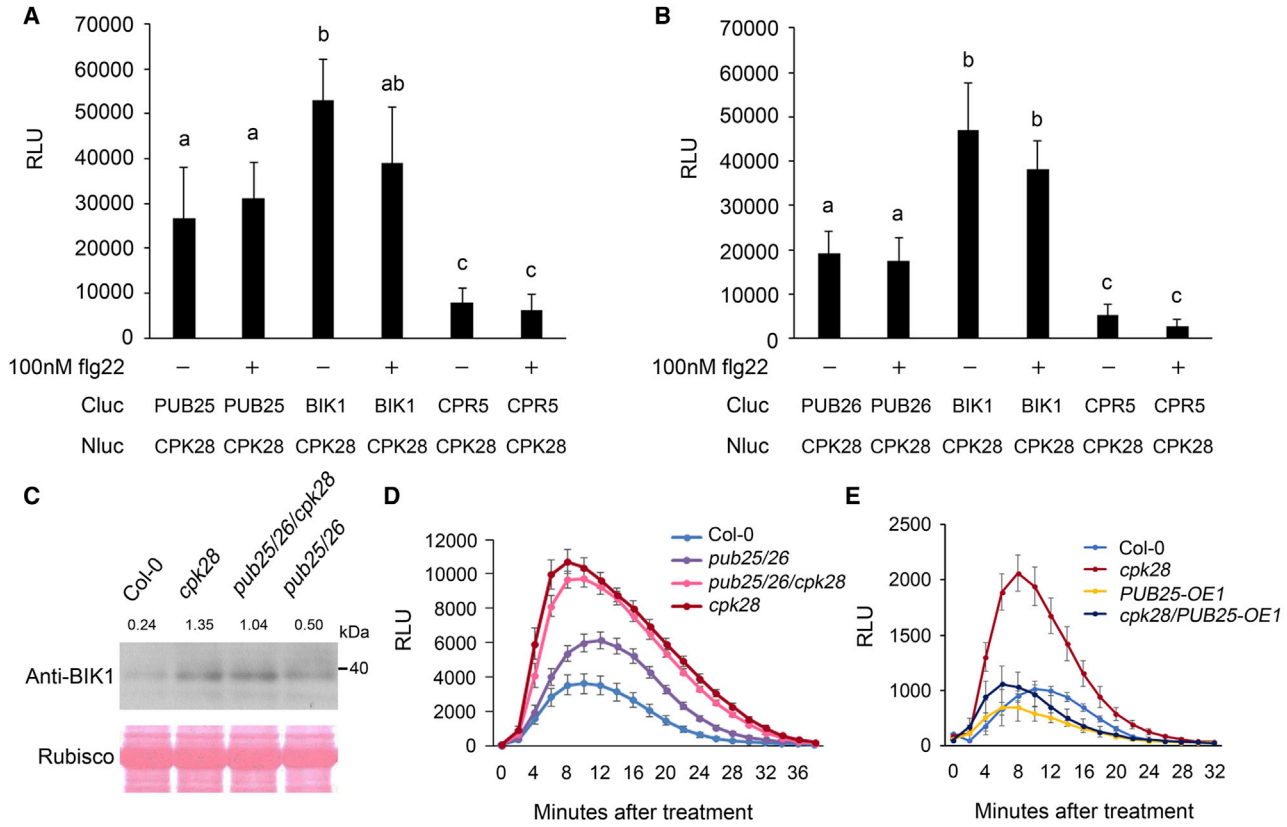

Figure 4. CPK28 Acts Together with PUB25/26 to Prevent Over-accumulation of BIK1 and Hyper-activation of Immunity

(A and B) CPK28 interacts with PUB25 (A) and PUB26 (B) in plants. Split-luciferase assays were conducted with the indicated constructs in *N. benthamiana* with or without 100 nM flg22 treatment. Values are means ± SDs (n = 12).

(C) *cpk28* and *pub25 pub26 cpk28* triple mutants over-accumulate BIK1. BIK1 protein was detected by immunoblot using anti-BIK1 antibodies. Ponceau S staining of Rubisco indicates equal loading. Numbers indicate arbitrary units of BIK1 calculated from densitometry measurements normalized to total Rubisco protein.

(D) *pub25 pub26*, *pub25 pub26 cpk28*, and *cpk28* mutants display elevated ROS burst in response to flg22. Values are mean relative light units (RLU) ± SDs (n = 8).

(E) Overexpression of *PUB25* (*PUB25-OE1*) in *cpk28* restores wild-type levels of flg22-induced ROS burst. Values are mean relative light units (RLU) ± SDs (n = 12).

Each experiment was repeated at least three times with similar results.

See also Figure S4.

flg22 often increased amounts of the slow-migrating form (Figures S1A and S1B). Incubation of protein samples with a protein phosphatase eliminated the slow-migrating forms (Figures S5A and S5B), indicating that PUB25/26 are phosphorylated following flg22 perception. We affinity-purified PUB26-FLAG from flg22-treated protoplasts and conducted LC-MS/MS analysis to identify phospho-peptides. In total, eight phospho-sites in PUB26-FLAG were identified, seven of which are conserved in PUB25 (Figure 5A). Site-directed mutagenesis was used to substitute each of these residues to alanine. The T94A mutation, but not T407A and S63A mutations, specifically abolished the flg22-induced band shift in PUB26 (Figure S5C). Mutation of the corresponding site in PUB25, T95A, similarly eliminated flg22-induced phosphorylation (Figure S5H). These results indicated that T95/94 are the main flg22-induced phospho-sites in PUB25/26, respectively. It is interesting to note that this threonine is in a typical CPK phosphorylation motif φXXXXTXB, where φ, X, T, and B represent a hydrophobic residue, any residue, threonine, and basic residue, respectively (Huang et al., 2001). This motif is also conserved in the related E3 ligases PUB22/23/24.

To test whether CPK28 and BIK1 are able to phosphorylate PUB25^{T95}/26^{T94}, we raised antibodies that specifically recognize an identical phospho-peptide spanning PUB25^{T95}/26^{T94} (Figure 5A; anti-pT94/95 antibodies). Immunoblot analyses detected strong phosphorylation of GST-PUB25/26 recombinant proteins at this site when incubated with GST-CPK28, but not HIS-BIK1 (Figures 5B and S5D). Importantly, the PUB25^{T95A}/26^{T94A} variants were not phosphorylated. Addition of the Ca^{2+} chelator EGTA to the reaction completely eliminated PUB26^{T94} phosphorylation (Figure S5E), a result consistent with Ca^{2+} dependency of CPK28 (Matschi et al., 2013; Bender et al., 2017). These data indicate that CPK28, but not BIK1, phosphorylates PUB25^{T95}/26^{T94}.

Anti-pT94/95 antibodies detected a strong phosphorylation on PUB25/26-FLAG affinity-purified from flg22-treated Col-0

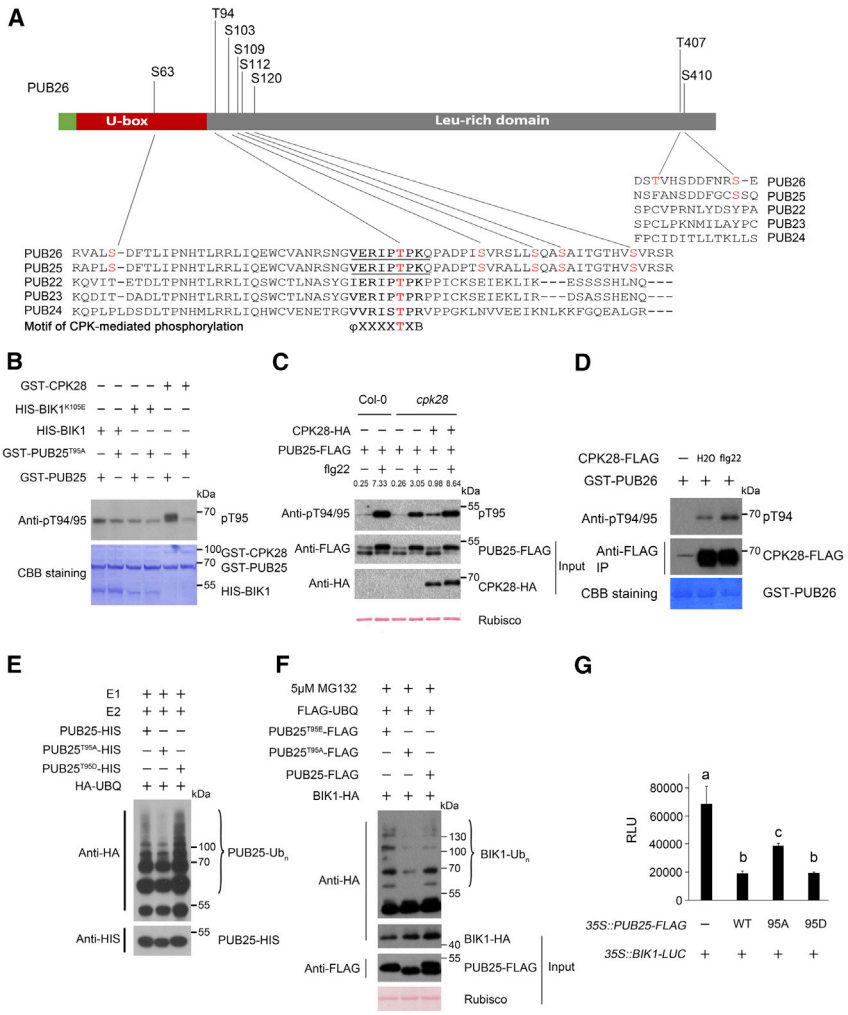

Figure 5. CPK28 Phosphorylates PUB25/26 to Enhance BIK1 Turnover and Dampen Immunity

(A) Schematic diagram of PUB26 phospho-sites. The PUB26-FLAG protein was affinity-purified from Col-0 protoplasts pretreated with 1 μM flg22 and subjected to phospho-peptide identification by LC-MS/MS. The identified phopho-sites were aligned to PUB22/23/24/25 amino acid sequences and shown below the schematic diagram. The underlined sequence was used to generate anti-pT94/95 antibodies. φXXXXTXB denotes a predicted CPK phosphorylation motif, where φ, X, B, and T represent a hydrophobic residue, any residue, basic residue, and threonine, respectively.

(B) CPK28, but not BIK1, phosphorylates PUB25^{T95}. Kinase assays were performed *in vitro* by incubating GST-PUB25 or GST-PUB25^{T95A} with HIS-BIK1, HIS-BIK1^{K105E}, and GST-CPK28. Protein phosphorylation was detected by anti-pT94/95 immunoblots. The fast-migrating band across all lanes was caused by background signal. Purified recombinant proteins were stained with Coomassie Brilliant Blue (CBB).

(C) Flg22 induces PUB25^{T95} phosphorylation in a manner partially dependent on *CPK28*. Protoplasts of the indicated genotypes were transfected with the indicated constructs and treated with or without 1 μM flg22 for 10 min before total protein was extracted. PUB25-FLAG protein was enriched by affinity purification, and PUB25^{T95} phosphorylation was detected by immunoblot using anti-pT94/95 antibodies (upper panel). Total PUB25-FLAG and CPK28-HA in the input were detected by anti-FLAG and anti-HA immunoblot, respectively (lower panels). Values indicate relative amounts of phosphorylated protein normalized to total PUB25-FLAG. Ponceau S staining of Rubisco indicates equal loading. Numbers indicate arbitrary units of PUB25^{T95} phosphorylation calculated from densitometry measurements normalized to total PUB25-FLAG protein (sum of upper and lower bands).

(D) Flg22 enhances CPK28 kinase activity in plants. *N. benthamiana* plants transiently expressing CPK28-FLAG were treated with flg22 or H_2O 20 min prior to protein isolation. CPK28-FLAG was then affinity-purified and incubated with the recombinant GST-PUB26 protein in the *in vitro* kinase buffer. PUB26 phosphorylation was detected by anti-pT94/95 immunoblots. Purified GST-PUB26 was stained with Coomassie Brilliant Blue (CBB).

(E) T95 phosphorylation enhances PUB25 E3 ligase activity. *In vitro* ubiquitination assays were performed with the indicated recombinant proteins, and PUB25 auto-ubiquitination was detected with immunoblot using an anti-HA antibody.

(F) PUB25^{T95} phosphorylation promotes BIK1 poly-ubiquitination. Col-0 protoplasts transfected with the indicated constructs were incubated overnight in the presence of 5 μM MG132. Ubiquitinated BIK1-HA was enriched with anti-FLAG beads and detected by anti-HA immunoblot. Ponceau S staining of Rubisco indicates equal loading.

(G) PUB25^{T95} phosphorylation positively regulates BIK1 degradation. The indicated constructs were transiently expressed in *N. benthamiana* plants, and luciferase activity was measured. Values are mean relative light units (RLU) ± SDs (n = 8). Different letters indicate significant difference at $p < 0.05$.

Each experiment was repeated twice (B and D) or at least three times (C and E–G) with similar results.

See also Figure S5 and Table S2.

protoplasts (Figures 5C and S5F), indicating flg22-induced phosphorylation of PUB25^{T95}/26^{T94} in the plant cell. This phosphorylation was reduced to ~40% for PUB25 and ~50% for PUB26 in *cpk28* protoplasts, whereas transfection of *cpk28* protoplasts restored the flg22-induced phosphorylation (Figures 5C and S5F), demonstrating that CPK28 is responsible for at least half of the phosphorylation *in vivo* and suggesting an induction of CPK28 activity by flg22. Indeed, the CPK28-FLAG protein reproducibly displayed a slight flg22-induced mobility shift in SDS-PAGE, which was eliminated upon phosphatase treatment (Figure S5G). CPK28-FLAG was transiently expressed in *N. benthamiana* plants to further test whether flg22 enhances CPK28 kinase activity. CPK28-FLAG isolated from the flg22-treated leaves phosphorylated *in vitro* the recombinant GST-PUB26 protein more strongly compared to H_2O treatment (Figure 5D), demonstrating that flg22 treatment indeed enhances CPK28 kinase activity in plants.

We next asked whether PUB25^{T95}/26^{T94} phosphorylation affects their function. CoIP assays showed that PUB25^{T95A}/26^{T94A}, PUB25^{T95D}/26^{T94D}, and wild-type PUB25/26 associated similarly with BIK1 (Figures S5H and S5I), suggesting that phosphorylation at this site does not affect PUB25/26-BIK1

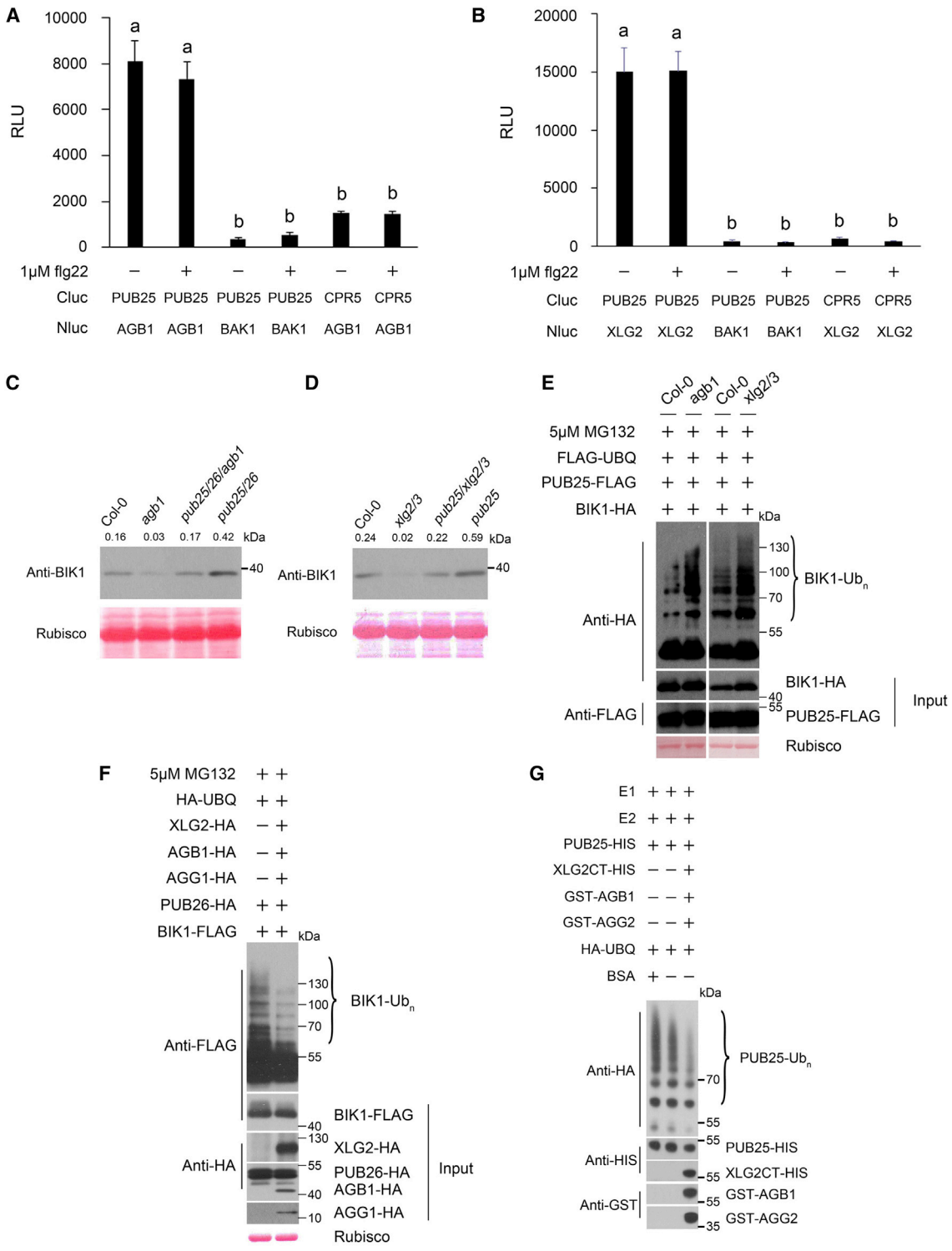

Figure 6. Heterotrimeric G Proteins Stabilize BIK1 by Directly Inhibiting PUB25 E3 Ligase Activity

(A and B) PUB25 interacts with AGB1 (A) and XLG2 (B) in plants. Split-luciferase assays were performed in *N. benthamiana* with the indicated constructs with or without 1 μM flg22 treatment. Values are means of relative light units (RLU) ± SDs (n = 8). Different letters indicate significant difference at $p < 0.05$.

(C and D) *pub25* and *pub26* mutations restore BIK1 accumulation in *agb1* (C) and *xlg2 xlg3* mutants (D). BIK1 levels in plants of the indicated genotypes were determined by immunoblot using anti-BIK1 antibodies; Ponceau S staining of Rubisco indicates equal loading. Numbers indicate arbitrary units of BIK1 calculated from densitometry measurements normalized to the Rubisco protein.

(legend continued on next page)

association. *In vitro* ubiquitination assays showed that auto-ubiquitination of PUB25^{T95A} and PUB25^{T95D} was notably decreased and enhanced, respectively (Figure 5E), suggesting that phosphorylation of PUB25^{T95} (and presumably PUB26^{T94}) is required for optimal E3 ligase activity. We further co-expressed PUB25-FLAG variants with BIK1-HA and FLAG-UBQ in protoplasts followed by MG132 treatment. Anti-HA immunoblot analyses showed that PUB25^{T95A} was much less capable of inducing BIK1 laddering compared to wild-type PUB25, whereas PUB25^{T95E} enhanced BIK1 laddering (Figure 5F). These results clearly demonstrated that T95 phosphorylation enhances PUB25 E3 ligase activity and promotes BIK1 poly-ubiquitination. To determine whether PUB25^{T95} phosphorylation promotes BIK1 degradation, a BIK1-LUC translational fusion reporter construct was generated, so that luciferase activity could be used as an indication of BIK1 protein level. Transient expression of this reporter construct along with PUB25-FLAG or PUB25^{T95D}-FLAG in *N. benthamiana* plants strongly reduced luciferase activity, a result indicative of BIK1 degradation caused by PUB25 (Figure 5G). Transient expression of PUB25^{T95A} also reduced luciferase activity compared to the control, but it was less pronounced compared to plants expressing the wild-type PUB25 (Figure 5G), indicating that the phosphorylation is required for optimum function of PUB25. Together, these results demonstrated that CPK28-mediated phosphorylation on PUB25^{T95}/26^{T94} promotes BIK1 degradation.

Since PUB25/26 target under-phosphorylated BIK1, we tested the impact of the *cpk28* mutation on the removal of non-activated BIK1 and accumulation of activated BIK1 following flg22 treatment. In Col-0 protoplasts, the levels of under-phosphorylated BIK1 rapidly decreased upon flg22 treatment and were reduced to ~13% within 20 min, whereas the hyper-phosphorylated BIK1 remained relatively steady between 10 and 40 min following flg22 treatment (Figures S5J and S5K). In contrast, the levels of under-phosphorylated BIK1 decreased more slowly in *cpk28* protoplasts. Accordingly, hyper-phosphorylated BIK1 accumulated to higher levels than in Col-0 protoplasts. The results suggested that CPK28 actively promotes depletion of under-phosphorylated BIK1, which in turn restricts the amount of hyper-phosphorylated BIK1 following flg22 perception.

Heterotrimeric G Proteins Directly Inhibit PUB25/26 E3 Ligase Activity

Heterotrimeric G proteins composed of XLG2/XLG3 (Gα), AGB1 (Gβ), and AGG1/AGG2 (Gγ) positively regulate BIK1 stability by attenuating proteasome-dependent degradation of BIK1 (Liang et al., 2016). Split-luciferase and coIP assays showed that PUB25/26 strongly associate with XLG2 and AGB1 irrespective of flg22 elicitation (Figures 6A, 6B, and S6A–S6D), indicating that PUB25/26 and heterotrimeric G proteins may act in the same pathway to regulate BIK1 stability. To test this, we generated *pub25 xlg2 xlg3* and *pub25 pub26 agb1* triple mutants. Consistent with previous findings (Liang et al., 2016), *agb1* and *xlg2 xlg3* plants accumulated less BIK1 compared to Col-0 plants (Figures 6C and 6D). The triple mutants were largely restored in BIK1 accumulation, indicating that PUB25/26 act downstream of the heterotrimeric G proteins.

Anti-HA immunoblots detected enhanced laddering signal in BIK1-HA isolated from *agb1* and *xlg2 xlg3* mutants compared to Col-0 protoplasts co-expressing PUB25-FLAG, FLAG-UBQ, and BIK1-HA (Figure 6E). Conversely, overexpression of HA-tagged heterotrimeric G proteins along with PUB26-HA and BIK1-FLAG in Col-0 protoplasts strongly diminished BIK1 laddering signal (Figure 6F). Together these results indicate that the heterotrimeric G proteins negatively regulate PUB25/26-mediated ubiquitination of BIK1.

CoIP experiments showed that PUB26 and BIK1 interacted normally in *agb1* mutant protoplasts (Figure S6E), suggesting that the G proteins regulate BIK1 ubiquitination independent of PUB26-BIK1 interaction. We next performed *in vitro* ubiquitination assays to test whether the G proteins directly inhibit PUB25 E3 ligase activity. Because the full-length XLG2 is membrane-associated and difficult to express in *E. coli*, we purified a HIS-tagged C-terminal half of XLG2 (XLG2CT) recombinant protein containing the Gα domain. We also purified GST-tagged full-length AGB1 and AGG2 recombinant proteins. Addition of the G proteins, but not BSA, to the reaction greatly reduced PUB25 auto-ubiquitination *in vitro* (Figure 6G), demonstrating that the heterotrimeric G proteins can directly inhibit PUB25 E3 ligase activity. Together, these results demonstrate that the heterotrimeric G proteins directly inhibit the E3 ligase activity of PUB25/26, resulting in reduced poly-ubiquitination and increased stability of BIK1.

DISCUSSION

Overall, our results demonstrate that PUB25/26 negatively regulate plant immunity by ubiquitinating and promoting degradation of BIK1 (Figure S6F). We also show that PUB25/26 are subject to positive and negative regulation by CPK28 and heterotrimeric G proteins, respectively. Thus PUB25/26, CPK28, and the heterotrimeric G proteins form a signaling module to control BIK1 accumulation and immune homeostasis.

Phosphorylation is known to regulate E3 ligases (Vierstra, 2003). PUB25/26 possess basal E3 ligase activity and catalyze

(E) Heterotrimeric G protein mutants display increased BIK1 poly-ubiquitination. The indicated constructs were expressed in protoplasts of the indicated genotype and incubated overnight in the presence of 5 μM MG132. Ubiquitinated BIK1-HA was purified with anti-FLAG beads. BIK1 ubiquitination was determined with anti-HA immunoblot. Ponceau S staining of Rubisco indicates equal loading.

(F) Overexpression of heterotrimeric G proteins inhibits BIK1 poly-ubiquitination in protoplasts. The indicated constructs were expressed in Col-0 protoplasts and incubated overnight in the presence of 5 μM MG132. Total BIK1-FLAG was affinity-purified with anti-FLAG beads. BIK1 ubiquitination was determined with anti-FLAG immunoblot. Ponceau S staining of Rubisco indicates equal loading.

(G) Recombinant heterotrimeric G proteins directly inhibit PUB25 auto-ubiquitination. *In vitro* ubiquitination assays were performed with the indicated recombinant proteins. BSA was added as a negative control. PUB25 auto-ubiquitination was determined by anti-HA immunoblot.

Each experiment was repeated at least twice (A–D) or three times (E–G) with similar results.

See also Figure S6.

poly-ubiquitination on BIK1. This activity is enhanced upon phosphorylation on T95/94, a site adjacent to the U-box, an E3 ligase catalytic domain (Cyr et al., 2002). It is conceivable that this residue may regulate E3 ligase activity through a phosphorylation-induced conformational change in the U-box domain (Buetow et al., 2016; Caulfield et al., 2014; Dou et al., 2012). Consistently, a phospho-dead mutation of this site attenuated PUB25-mediated BIK1 degradation in *N. benthamiana*.

Several lines of evidence support that CPK28 acts together with PUB25/26 to regulate BIK1 stability and immunity. CPK28 interacts with and directly phosphorylates PUB25^{T95}/26^{T94}. The *cpk28 pub25 pub26* triple mutant and the *cpk28* single mutant are near identical in terms of BIK1 protein accumulation and flg22-induced ROS production, indicating that CPK28 and PUB25/26 act in the same pathway. The related E3 ligases PUB22/23/24 may also destabilize BIK1 downstream of CPK28, as we show that they contain the conserved CPK phospho-site and that PUB22/23 can destabilize BIK1. Indeed, PUB22/23/24 are known to negatively regulate immunity (Trujillo et al., 2008). These findings explain greater amounts of BIK1 level and stronger immune responses in *cpk28* plants than that in *pub25 pub26* plants.

The *cpk28* mutant constitutively accumulates higher levels of BIK1 protein (Monaghan et al., 2014), suggesting that CPK28 regulates BIK1 stability in the resting state. A recent report showed that a recombinant, phosphorylated form of CPK28 is already fully activated *in vitro* at low Ca^{2+} concentrations (Bender et al., 2017). Our results suggest that the flg22-induced phosphorylation of PUB25^{T95}/26^{T94} is partially mediated by CPK28. Although previous in-gel kinase assays failed to detect an altered CPK28 phosphorylation state after flg22 treatment (Monaghan et al., 2015), the reduced CPK28 mobility in SDS-PAGE and increased CPK28 kinase activity upon flg22 treatment observed in this study support that CPK28 further destabilizes BIK1 following flg22 treatment. Understanding the mechanism of CPK28 activation is an interesting area of future research.

Our analyses of PUB25/26 further uncovered two mechanisms through which BIK1 stability is actively maintained both before and after pattern recognition (Figure S6F). First, heterotrimeric G proteins interact with PUB25/26 to inhibit their E3 ligase activity, explaining our previous finding that they positively regulate BIK1 stability and pattern-triggered immunity (Liang et al., 2016). Second, PUB25/26 selectively target under-phosphorylated BIK1 for degradation. Flg22-induced S236/T237 phosphorylation in the activation loop protects BIK1 from PUB25/26-mediated poly-ubiquitination and degradation. This phosphorylation may induce a conformational change in BIK1 that masks the poly-ubiquitination site, a possibility that awaits structural studies. Nonetheless, this mechanism contrasts the reported degradation of FLS2 by PUB12/13, which target activated FLS2 for degradation (Lu et al., 2011), but is similar to the SINAT E3 ligase-mediated ubiquitination and degradation of dephosphorylated BES1 in BR signaling (Yang et al., 2017). Activation of the FLS2-BIK1 complex sets into motion immune signaling cascades that are required to protect plant cells from infection. To prevent excessive signaling and maintain homeostasis, we propose that any under-phosphorylated BIK1 is degraded by PUB25/26 to deplete the pool of signal-competent BIK1.

Regulated degradation of key signaling components allows plants to respond to environmental signals with speed and robustness, but with controlled duration and amplitude. This can be achieved by recruitment of E3 ligases and is often described as an "on-off" switch (Ding et al., 2015; Dong et al., 2017; Lu et al., 2011; Ni et al., 2014; Spoel et al., 2009). Our findings show how PUB25/26-mediated degradation of BIK1 is dynamically controlled by multiple mechanisms (Figure S6F). In the resting state, BIK1 exists primarily in an under-phosphorylated pool. The countering activities of CPK28 and heterotrimeric G proteins on PUB25/26 maintain BIK1 homeostasis to ensure robust yet appropriate immune activation upon pathogen attack. Following activation by flg22, the FLS2 complex phosphorylates BIK1 to form an activated pool. Flg22 treatment additionally induces dissociation of the G proteins from the FLS2-BIK1 complex (Liang et al., 2016) and increased phosphorylation of PUB25/26 by CPK28. These are expected to rapidly deplete the under-phosphorylated pool and prevent further accumulation of activated BIK1, thereby controlling the amplitude of immune responses. Thus, heterotrimeric G proteins, CPK28, and PUB25/26 form a regulatory module for BIK1 accumulation crucial for plant immune signaling homeostasis.

STAR★METHODS

Detailed methods are provided in the online version of this paper and include the following:

- KEY RESOURCES TABLE
- CONTACT FOR REAGENT AND RESOURCE SHARING
- EXPERIMENTAL MODEL AND SUBJECT DETAILS
  - Plant Materials and Growth Conditions
- METHOD DETAILS
  - Constructs and Transgenic Plants
  - Oxidative Burst Assay
  - Pathogen Inoculation and Disease Resistance Assays
  - Split-Luciferase Assay
  - Co-Immunoprecipitation Assay
  - *In Vitro* Ubiquitination Assay
  - Ubiquitination Assay in Protoplasts
  - BIK1 Protein Stability in Protoplasts
  - Protein Degradation Assay in *N. benthamiana* Plants
  - LC-MS/MS Analysis
  - Generation of Antibodies
  - *In Vitro* Phosphorylation Assays
- QUANTIFICATION AND STATISTICAL ANALYSIS

SUPPLEMENTAL INFORMATION

Supplemental Information includes six figures and three tables and can be found with this article online at https://doi.org/10.1016/j.molcel.2017.12.026.

ACKNOWLEDGMENTS

The work was supported by grants from the Chinese Natural Science Foundation (31521001), the Strategic Priority Research Program of the Chinese Academy of Sciences (grant no. XDB11020200), and the State Key Laboratory of Plant Genomics (SKLPG2016B-2) to J.-M.Z., as well as a Discovery Grant from the Natural Sciences and Engineering Research Council of Canada (NSERC) and start-up funds from Queen's University to J.M., and by the

Gatsby Charitable Foundation and the European Research Council (grant "PHOSPHinnATE") to C.Z. L.E.G. was supported by an NSERC Undergraduate Summer Research Award (USRA), an NSERC Canada Graduate Scholarship for Master's Students (CGS-M), and an Ontario Graduate Scholarship (OGS).

AUTHOR CONTRIBUTIONS

Jinlong Wang, J.M., and J.-M.Z. designed the study. Jinlong Wang, L.E.G., Jiayu Wang, X.L., Lin Li, C.G., M.M., F.F., M.L., Lei Li, X.Z., and F.Y. performed the experiments. Jinlong Wang, Q.X., S.C., J.M., and J.-M.Z. analyzed the data. Jinlong Wang, C.Z., J.M., and J.-M.Z. wrote the paper.

DECLARATION OF INTERESTS

The authors declare no competing interests.

Received: June 1, 2017
Revised: October 19, 2017
Accepted: December 22, 2017
Published: January 18, 2018

REFERENCES

Bender, K.W., Blackburn, R.K., Monaghan, J., Derbyshire, P., Menke, F.L., Zipfel, C., Goshe, M.B., Zielinski, R.E., and Huber, S.C. (2017). Autophosphorylation-based calcium (Ca^{2+}) sensitivity priming and Ca^{2+}/calmodulin inhibition of *Arabidopsis thaliana* Ca^{2+}-dependent protein kinase 28 (CPK28). J. Biol. Chem. *292*, 3988–4002.

Buetow, L., Tria, G., Ahmed, S.F., Hock, A., Dou, H., Sibbet, G.J., Svergun, D.I., and Huang, D.T. (2016). Casitas B-lineage lymphoma linker helix mutations found in myeloproliferative neoplasms affect conformation. BMC Biol. *14*, 76.

Caulfield, T.R., Fiesel, F.C., Moussaud-Lamodière, E.L., Dourado, D.F., Flores, S.C., and Springer, W. (2014). Phosphorylation by PINK1 releases the UBL domain and initializes the conformational opening of the E3 ubiquitin ligase Parkin. PLoS Comput. Biol. *10*, e1003935.

Chen, H., Zou, Y., Shang, Y., Lin, H., Wang, Y., Cai, R., Tang, X., and Zhou, J.M. (2008). Firefly luciferase complementation imaging assay for protein-protein interactions in plants. Plant Physiol. *146*, 368–376.

Choe, S., Fujioka, S., Noguchi, T., Takatsuto, S., Yoshida, S., and Feldmann, K.A. (2001). Overexpression of *DWARF4* in the brassinosteroid biosynthetic pathway results in increased vegetative growth and seed yield in *Arabidopsis*. Plant J. *26*, 573–582.

Couto, D., Niebergall, R., Liang, X., Bücherl, C.A., Sklenar, J., Macho, A.P., Ntoukakis, V., Derbyshire, P., Altenbach, D., Maclean, D., et al. (2016). The *Arabidopsis* protein phosphatase PP2C38 negatively regulates the central immune kinase BIK1. PLoS Pathog. *12*, e1005811.

Cyr, D.M., Höhfeld, J., and Patterson, C. (2002). Protein quality control: U-box-containing E3 ubiquitin ligases join the fold. Trends Biochem. Sci. *27*, 368–375.

Ding, L., Pandey, S., and Assmann, S.M. (2008). *Arabidopsis* extra-large G proteins (XLGs) regulate root morphogenesis. Plant J. *53*, 248–263.

Ding, Y., Li, H., Zhang, X., Xie, Q., Gong, Z., and Yang, S. (2015). OST1 kinase modulates freezing tolerance by enhancing ICE1 stability in *Arabidopsis*. Dev. Cell *32*, 278–289.

Dong, H., Dumenil, J., Lu, F.H., Na, L., Vanhaeren, H., Naumann, C., Klecker, M., Prior, R., Smith, C., McKenzie, N., et al. (2017). Ubiquitylation activates a peptidase that promotes cleavage and destabilization of its activating E3 ligases and diverse growth regulatory proteins to limit cell proliferation in *Arabidopsis*. Genes Dev. *31*, 197–208.

Dou, H., Buetow, L., Hock, A., Sibbet, G.J., Vousden, K.H., and Huang, D.T. (2012). Structural basis for autoinhibition and phosphorylation-dependent activation of c-Cbl. Nat. Struct. Mol. Biol. *19*, 184–192.

Feng, F., and Zhou, J.M. (2012). Plant-bacterial pathogen interactions mediated by type III effectors. Curr. Opin. Plant Biol. *15*, 469–476.

Feng, F., Yang, F., Rong, W., Wu, X., Zhang, J., Chen, S., He, C., and Zhou, J.M. (2012). A *Xanthomonas* uridine 5′-monophosphate transferase inhibits plant immune kinases. Nature *485*, 114–118.

Holsters, M., Silva, B., Van Vliet, F., Genetello, C., De Block, M., Dhaese, P., Depicker, A., Inzé, D., Engler, G., Villarroel, R., et al. (1980). The functional organization of the nopaline *A. tumefaciens* plasmid pTiC58. Plasmid *3*, 212–230.

Huang, J.Z., Hardin, S.C., and Huber, S.C. (2001). Identification of a novel phosphorylation motif for CDPKs: phosphorylation of synthetic peptides lacking basic residues at P-3/P-4. Arch. Biochem. Biophys. *393*, 61–66.

Kadota, Y., Sklenar, J., Derbyshire, P., Stransfeld, L., Asai, S., Ntoukakis, V., Jones, J.D.G., Shirasu, K., Menke, F., Jones, A., and Zipfel, C. (2014). Direct regulation of the NADPH oxidase RBOHD by the PRR-associated kinase BIK1 during plant immunity. Mol. Cell *54*, 43–55.

Kong, Q., Sun, T., Qu, N., Ma, J., Li, M., Cheng, Y.T., Zhang, Q., Wu, D., Zhang, Z., and Zhang, Y. (2016). Two redundant receptor-like cytoplasmic kinases function downstream of pattern recognition receptors to regulate activation of SA biosynthesis. Plant Physiol. *171*, 1344–1354.

Li, X., Lin, H., Zhang, W., Zou, Y., Zhang, J., Tang, X., and Zhou, J.M. (2005). Flagellin induces innate immunity in nonhost interactions that is suppressed by *Pseudomonas syringae* effectors. Proc. Natl. Acad. Sci. USA *102*, 12990–12995.

Li, L., Li, M., Yu, L., Zhou, Z., Liang, X., Liu, Z., Cai, G., Gao, L., Zhang, X., Wang, Y., et al. (2014). The FLS2-associated kinase BIK1 directly phosphorylates the NADPH oxidase RbohD to control plant immunity. Cell Host Microbe *15*, 329–338.

Liang, X., Ding, P., Lian, K., Wang, J., Ma, M., Li, L., Li, L., Li, M., Zhang, X., Chen, S., et al. (2016). *Arabidopsis* heterotrimeric G proteins regulate immunity by directly coupling to the FLS2 receptor. eLife *5*, e13568.

Lin, W., Lu, D., Gao, X., Jiang, S., Ma, X., Wang, Z., Mengiste, T., He, P., and Shan, L. (2013). Inverse modulation of plant immune and brassinosteroid signaling pathways by the receptor-like cytoplasmic kinase BIK1. Proc. Natl. Acad. Sci. USA *110*, 12114–12119.

Liu, J., Elmore, J.M., Lin, Z.J., and Coaker, G. (2011). A receptor-like cytoplasmic kinase phosphorylates the host target RIN4, leading to the activation of a plant innate immune receptor. Cell Host Microbe *9*, 137–146.

Lu, D., Wu, S., Gao, X., Zhang, Y., Shan, L., and He, P. (2010). A receptor-like cytoplasmic kinase, BIK1, associates with a flagellin receptor complex to initiate plant innate immunity. Proc. Natl. Acad. Sci. USA *107*, 496–501.

Lu, D., Lin, W., Gao, X., Wu, S., Cheng, C., Avila, J., Heese, A., Devarenne, T.P., He, P., and Shan, L. (2011). Direct ubiquitination of pattern recognition receptor FLS2 attenuates plant innate immunity. Science *332*, 1439–1442.

Macho, A.P., and Zipfel, C. (2015). Targeting of plant pattern recognition receptor-triggered immunity by bacterial type-III secretion system effectors. Curr. Opin. Microbiol. *23*, 14–22.

Matschi, S., Werner, S., Schulze, W.X., Legen, J., Hilger, H.H., and Romeis, T. (2013). Function of calcium-dependent protein kinase CPK28 of *Arabidopsis thaliana* in plant stem elongation and vascular development. Plant J. *73*, 883–896.

Monaghan, J., Matschi, S., Shorinola, O., Rovenich, H., Matei, A., Segonzac, C., Malinovsky, F.G., Rathjen, J.P., MacLean, D., Romeis, T., and Zipfel, C. (2014). The calcium-dependent protein kinase CPK28 buffers plant immunity and regulates BIK1 turnover. Cell Host Microbe *16*, 605–615.

Monaghan, J., Matschi, S., Romeis, T., and Zipfel, C. (2015). The calcium-dependent protein kinase CPK28 negatively regulates the BIK1-mediated PAMP-induced calcium burst. Plant Signal. Behav. *10*, e1018497.

Ni, W., Xu, S.L., Tepperman, J.M., Stanley, D.J., Maltby, D.A., Gross, J.D., Burlingame, A.L., Wang, Z.Y., and Quail, P.H. (2014). A mutually assured destruction mechanism attenuates light signaling in *Arabidopsis*. Science *344*, 1160–1164.

Niu, Y., and Sheen, J. (2012). Transient expression assays for quantifying signaling output. Methods Mol. Biol. *876*, 195–206.

Ranf, S., Eschen-Lippold, L., Fröhlich, K., Westphal, L., Scheel, D., and Lee, J. (2014). Microbe-associated molecular pattern-induced calcium signaling requires the receptor-like cytoplasmic kinases, PBL1 and BIK1. BMC Plant Biol. *14*, 374.

Shi, H., Shen, Q., Qi, Y., Yan, H., Nie, H., Chen, Y., Zhao, T., Katagiri, F., and Tang, D. (2013). BR-SIGNALING KINASE1 physically associates with FLAGELLIN SENSING2 and regulates plant innate immunity in *Arabidopsis*. Plant Cell *25*, 1143–1157.

Spoel, S.H., Mou, Z., Tada, Y., Spivey, N.W., Genschik, P., and Dong, X. (2009). Proteasome-mediated turnover of the transcription coactivator NPR1 plays dual roles in regulating plant immunity. Cell *137*, 860–872.

Tang, D., Wang, G., and Zhou, J.M. (2017). Receptor kinases in plant pathogen interactions: more than pattern recognition. Plant Cell *29*, 618–637.

Trujillo, M., Ichimura, K., Casais, C., and Shirasu, K. (2008). Negative regulation of PAMP-triggered immunity by an E3 ubiquitin ligase triplet in *Arabidopsis*. Curr. Biol. *18*, 1396–1401.

Ullah, H., Chen, J.G., Temple, B., Boyes, D.C., Alonso, J.M., Davis, K.R., Ecker, J.R., and Jones, A.M. (2003). The beta-subunit of the *Arabidopsis* G protein negatively regulates auxin-induced cell division and affects multiple developmental processes. Plant Cell *15*, 393–409.

Vierstra, R.D. (2003). The ubiquitin/26S proteasome pathway, the complex last chapter in the life of many plant proteins. Trends Plant Sci. *8*, 135–142.

Wang, Z.Y., Seto, H., Fujioka, S., Yoshida, S., and Chory, J. (2001). BRI1 is a critical component of a plasma-membrane receptor for plant steroids. Nature *410*, 380–383.

Wang, G., Roux, B., Feng, F., Guy, E., Li, L., Li, N., Zhang, X., Lautier, M., Jardinaud, M.F., Chabannes, M., et al. (2015). The decoy substrate of a pathogen effector and a pseudokinase specify pathogen-induced modified-self recognition and immunity in plants. Cell Host Microbe *18*, 285–295.

Yamada, K., Yamaguchi, K., Shirakawa, T., Nakagami, H., Mine, A., Ishikawa, K., Fujiwara, M., Narusaka, M., Narusaka, Y., Ichimura, K., et al. (2016). The *Arabidopsis* CERK1-associated kinase PBL27 connects chitin perception to MAPK activation. EMBO J. *35*, 2468–2483.

Yang, M., Li, C., Cai, Z., Hu, Y., Nolan, T., Yu, F., Yin, Y., Xie, Q., Tang, G., and Wang, X. (2017). SINAT E3 ligases control the light-mediated stability of the brassinosteroid-activated transcription factor BES1 in *Arabidopsis*. Dev. Cell *41*, 47–58.e4.

Yuan, J., and He, S.Y. (1996). The *Pseudomonas syringae* Hrp regulation and secretion system controls the production and secretion of multiple extracellular proteins. J. Bacteriol. *178*, 6399–6402.

Zhang, J., Shao, F., Li, Y., Cui, H., Chen, L., Li, H., Zou, Y., Long, C., Lan, L., Chai, J., et al. (2007). A *Pseudomonas syringae* effector inactivates MAPKs to suppress PAMP-induced immunity in plants. Cell Host Microbe *1*, 175–185.

Zhang, J., Li, W., Xiang, T., Liu, Z., Laluk, K., Ding, X., Zou, Y., Gao, M., Zhang, X., Chen, S., et al. (2010). Receptor-like cytoplasmic kinases integrate signaling from multiple plant immune receptors and are targeted by a *Pseudomonas syringae* effector. Cell Host Microbe *7*, 290–301.

Zhao, Q., Liu, L., and Xie, Q. (2012). In vitro protein ubiquitination assay. Methods Mol. Biol. *876*, 163–172.

Zipfel, C., and Oldroyd, G.E. (2017). Plant signalling in symbiosis and immunity. Nature *543*, 328–336.

Zipfel, C., Robatzek, S., Navarro, L., Oakeley, E.J., Jones, J.D.G., Felix, G., and Boller, T. (2004). Bacterial disease resistance in *Arabidopsis* through flagellin perception. Nature *428*, 764–767.

STAR★METHODS

KEY RESOURCES TABLE

REAGENT or RESOURCE	SOURCE	IDENTIFIER
Antibodies		
Mouse monoclonal anti-GST	TIANGEN	Cat#AB101-02
Mouse monoclonal anti-HA	CWBIO	Cat#CW0092M
Mouse monoclonal anti-HIS	Sigma	Cat#H1029
Mouse monoclonal ANTI-FLAG M2	Sigma	Cat#F1804
Rabbit polyclonal anti-ACTIN	EASYBIO	Cat#BE0027-100
Rabbit polyclonal anti-BIK1	This paper	N/A
Rabbit polyclonal anti-FLS2	Zhang et al. (2010)	N/A
Rabbit polyclonal anti-pT94/T95	This paper	N/A
Bacterial and Virus Strains		
Agrobacterium tumefaciens GV3101	Holsters et al. (1980)	N/A
Botrytis cinerea	Institute of Plant Protection, Chinese Academy of Agricultural Sciences	N/A
Escherichia coli BL21	TransGen Biotech	Cat#CD901-03
Escherichia coli DH5α	CWBIO	Cat#CW0808S
Pseudomonas syringae pv *tomato* (*Pto*) DC3000 *hrcC*-	Yuan and He (1996)	N/A
Chemicals, Peptides, and Recombinant Proteins		
3 × FLAG peptide	Sigma	Cat#F4799
Anti-Flag M2 Beads (affinity gel)	Sigma	Cat#A2220
Cycloheximide (CHX)	Sigma-Aldrich	Cat#R750107
D-Luciferin	BioVision	Cat#7903
Flg22 peptides	Sangon Biotech	Custom order
Glutathione Sepharose 4 (affinity gel)	GE Healthcare	Cat#17-0756-01
HA-Ubiquitin (HA-UBQ)	R&D Systems	Cat#U-110
Luminol	Fluka	Cat#09253
MG132	Sigma	Cat#C2211
Ni-NTA Agarose (affinity gel)	QIAGEN	Cat#30210
Peroxidase	Sigma	Cat#P6782
PPase	NEB	Cat#P0753L
Sequencing grade trypsin	Sigma	Cat#T6567
Protease Inhibitor Cocktail Tablets	Roche	Cat#04693116001
Critical Commercial Assays		
Gateway LR Clonase II Enzyme Mix	Invitrogen	Cat#11791100
pENTR/D-TOPO Cloning Kit	Invitrogen	Cat#K240020SP
Experimental Models: Organisms/Strains		
Arabidopsis: 35S:PUB25-FLAG (PUB25-OE)	This paper	N/A
Arabidopsis: 35S:PUB25-FLAG-1 pBIK1::BIK1-HA	This paper	N/A
Arabidopsis: 35S:PUB26-FLAG (PUB26-OE)	This paper	N/A
Arabidopsis: agb1-2	Ullah et al. (2003)	N/A
Arabidopsis: cpk28 35S:PUB25-FLAG-1	This paper	N/A

(*Continued on next page*)

Continued

REAGENT or RESOURCE	SOURCE	IDENTIFIER
Arabidopsis: cpk28-1 (*GK-523B08*)	Monaghan et al. (2014)	N/A
Arabidopsis: pBIK1::BIK1-HA	Zhang et al. (2010)	N/A
Arabidopsis: pub25-1 (*SALK_147032*)	NASC	N/A
Arabidopsis: pub25-1 pub26-1	This paper	N/A
Arabidopsis: pub25-1 pub26-1 agb1-2	This paper	N/A
Arabidopsis: pub25-1 pub26-1 cpk28-1	This paper	N/A
Arabidopsis: pub25-1 xlg2-1 xlg3-1	This paper	N/A
Arabidopsis: pub26-1 (*GABI_308D07*)	NASC	N/A
Arabidopsis: pub26-2 (*GABI_270G01*)	NASC	N/A
Arabidopsis: xlg2-1 xlg3-1	Ding et al. (2008)	N/A
Oligonucleotides		
Primers see Table S3	Sangon Biotech	Custom order
Recombinant DNA		
pET28a	EMD Biosciences	69864-3
pGEX 6P-1	Amersham Biosciences	27-4597-01
pENTR	Invitrogen	K2400-20
pFAST-G01	Funakashi	IN3-VEC31
pCAMBIA1300	The Centre for Application of Molecular Biology to International Agriculture	N/A
pCAMBIA-35S:PUB25-FLAG	This paper	N/A
pCAMBIA-35S:PUB26-FLAG	This paper	N/A
pCAMBIA-35S-AGB1-HA-Nluc	Liang et al. (2016)	N/A
pCAMBIA-35S-BAK1-HA-Nluc	Liang et al. (2016)	N/A
pCAMBIA-35S-Cluc-BIK1	Liang et al. (2016)	N/A
pCAMBIA-35S-BIK1-HA-Nluc	Liang et al. (2016)	N/A
pCAMBIA-35S-CPK28-HA-Nluc	This paper	N/A
pCAMBIA-35S-Cluc-CPR5	Liang et al. (2016)	N/A
pCAMBIA-35S-PBL20-HA-Nluc	This paper	N/A
pCAMBIA-35S-Cluc-PUB25	This paper	N/A
pCAMBIA-35S-Cluc-PUB26	This paper	N/A
pCAMBIA-35S-XLG2-HA-Nluc	Liang et al. (2016)	N/A
pCAMBIA-pBIK1:BIK1-HA	Zhang et al. (2010)	N/A
pET28a-HIS-BIK1	Liang et al. (2016)	N/A
pET28a-HIS-BIK1^{K105E}	Liang et al. (2016)	N/A
pET28a-HIS-E1 (GI: 136632)	Qi Xie, Institute of Genetics and Developmental Biology	N/A
pET28a-HIS-UBC8	Qi Xie, Institute of Genetics and Developmental Biology	N/A
pET28a-PUB25^{T95A}-HIS	This paper	N/A
pET28a-PUB25^{T95D}-HIS	This paper	N/A
pET28a-PUB25-HIS	This paper	N/A
pET28a-PUB25-FLAG-HIS	This paper	N/A
pET28a-XLG2CT-HIS	Liang et al. (2016)	N/A

(*Continued on next page*)

Continued

REAGENT or RESOURCE	SOURCE	IDENTIFIER
pGEX6P.1-GST-AGB1	Liang et al. (2016)	N/A
pGEX6P.1-GST-AGG2	Liang et al. (2016)	N/A
pGEX6P.1-GST-BIK1	Zhang et al. (2010)	N/A
pGEX6P.1-GST-CPK28	This paper	N/A
pGEX6P.1-GST-PUB25	This paper	N/A
pGEX6P.1-GST-PUB25^{T95A}	This paper	N/A
pGEX6P.1-GST-PUB26	This paper	N/A
pGEX6P.1-GST-PUB26^{T95A}	This paper	N/A
pUC19-35S-FLAG-RBS	Li et al., (2005)	N/A
pUC19-35S-HA-RBS	Li et al., (2005)	N/A
pUC19-35S-AGB1-FLAG	Liang et al. (2016)	N/A
pUC19-35S-AGB1-HA	Liang et al. (2016)	N/A
pUC19-35S-AGG1-HA	Liang et al. (2016)	N/A
pUC19-35S-BIK1^{2A}-FLAG-RBS	This paper	N/A
pUC19-35S-BIK1^{2A}-HA	This paper	N/A
pUC19-35S-BIK1^{2D}-FLAG	This paper	N/A
pUC19-35S-BIK1^{2D}-HA	This paper	N/A
pUC19-35S-BIK1-FLAG	Zhang et al. (2010)	N/A
pUC19-35S-BIK1-HA	Zhang et al. (2010)	N/A
pUC19-35S-BIK1^{K105E}-HA	Zhang et al. (2010)	N/A
pUC19-35S-CPK28-HA	This paper	N/A
pUC19-35S-HA-UBQ	This paper	N/A
pUC19-35S-FLAG-UBQ	This paper	N/A
pUC19-35S-PUB25-FLAG	This paper	N/A
pUC19-35S-PUB25-HA	This paper	N/A
pUC19-35S-PUB25^{T95A}-FLAG	This paper	N/A
pUC19-35S-PUB25^{T95D}-FLAG	This paper	N/A
pUC19-35S-PUB26-FLAG	This paper	N/A
pUC19-35S-PUB26-HA	This paper	N/A
pUC19-35S-PUB26^{T94A}-FLAG	This paper	N/A
pUC19-35S-PUB26^{T94D}-FLAG	This paper	N/A
pUC19-35S-XLG2-FLAG	Liang et al. (2016)	N/A
pUC19-35S-XLG2-HA	Liang et al. (2016)	N/A
pUC19-PUB26^{S63A}-FLAG	This paper	N/A
pUC19-PUB26^{T407A}-FLAG	This paper	N/A
pUC19-PUB26^{T95A}-FLAG	This paper	N/A
Software and Algorithms		
IBM SPSS Statistics 22	IBM	https://www.ibm.com/analytics/cn/zh/technology/spss/

CONTACT FOR REAGENT AND RESOURCE SHARING

Further information and requests for reagents may be directed to and will be fulfilled by the Lead Contact, Jian-Min Zhou (jmzhou@genetics.ac.cn).

EXPERIMENTAL MODEL AND SUBJECT DETAILS

Plant Materials and Growth Conditions

Arabidopsis and *N. benthamiana* plants were grown on soil at 23/21°C day/night and 70% relative humidity with 10/14 h light/dark photoperiod. *Arabidopsis* materials used in this study are all derived from Col-0. Previously published lines include: *cpk28-1* (Matschi

et al., 2013; Monaghan et al., 2014), *xlg2-1 xlg3-1* (Ding et al., 2008), *agb1-2* (Ullah et al., 2003), *NP::BIK1-HA* (Zhang et al., 2010). T-DNA insertion mutants *pub25-1* (SALK_147032), *pub26-1* (GABI_308D07) and *pub26-2* (GABI_270G01) were obtained from the Nottingham *Arabidopsis* Stock Centre (NASC), and homozygous lines were obtained by genotyping using allele-specific primers. Additional *Arabidopsis* transgenic lines and higher order mutants generated in this study are described below. *35S::PUB25-FLAG* and *35S::PUB26-FLAG* were introduced into Col-0 plants to generate *PUB25/26* overexpression lines (*PUB25/26-OE*) using standard protocols. *PUB25-OE1/NP::BIK1-HA, PUB25-OE1/cpk28-1, pub25-1 pub26-1*, *pub25-1 xlg2-1 xlg3-1*, *pub25-1 pub26-1 agb1-2* and *pub25-1 pub26-1 cpk28-1* were generated in this study by crossing and confirmed by allele-specific genotyping, presence of transgenic antibiotic resistance, and/or immunoblotting.

METHOD DETAILS

Constructs and Transgenic Plants

Constructs for protoplast transfection experiments were generated by PCR-amplifying coding sequences from cDNA and inserting into the PUC19-35S-FLAG-RBS and PUC19-35S-HA-RBS vectors (Li et al., 2005).

To generate constructs for split-luciferase assays, coding sequences were PCR-amplified from cDNA and inserted into pCAMBIA-Cluc, pCAMBIA-Nluc or pCAMBIA-HA-Nluc (Chen et al., 2008; Liang et al., 2016).

To generate constructs for recombinant proteins, coding sequences were inserted into pGex6p.1 (Amersham Biosciences) or pET28a vectors (EMD Biosciences) to create translational fusion to GST and HIS tags, respectively.

To generate *PUB25/26-OE* transgenic plants, *35S::PUB25/26-FLAG* fragments were excised from the PUC19-35S-PUB25/26-FLAG constructs and cloned into the pCAMBIA1300 plasmid (The Centre for Application of Molecular Biology to International Agriculture, Canberra). The resulting constructs were introduced into Col-0 plants by *Agrobacterium*-mediated transformation using standard protocols.

To generate *PUB25-OE/NP::BIK1-HA* plants, the *PUB25-OE1* transgenic line was crossed with *NP::BIK1-HA* (Zhang et al., 2010), and sibling transgenic lines carrying both *PUB25-OE1* and *NP::BIK1-HA* transgenes or only the *NP::BIK1-HA* transgene were identified by immunoblot.

Point mutations were introduced into above constructs by site-directed mutagenesis. Primers used for construction and genotyping are listed in Table S3.

Oxidative Burst Assay

Leaves of 25-day-old-plants were sliced into approximately 1 mm^2 strips and floated overnight on sterile water in a 96-well plate. The following day the water was replaced with a solution of 20 mM luminol (Sigma) and 10 mg/mL horseradish peroxidase (Sigma) containing 1 μM flg22 (Zhang et al., 2007). Luminescence was captured by using GLOMAX 96 microplate luminometer (Promega). Alternatively, 4 mm-diameter leaf discs were collected from 4-5 week-old plants into 96-well plates as described previously (Monaghan et al., 2014), treated with 100 nM flg22 (EZ Biolabs), and luminescence recorded on a SpectraMax plate reader outfitted with the LUM module.

Pathogen Inoculation and Disease Resistance Assays

B. cinerea was cultured on potato dextrose agar (PDA) medium (200 g/L Potato, 20 g/L Glucose, 15 g/L Agar) and incubated at 24°C with a 12 hr photoperiod. Conidia were collected by flooding the plates using distilled water, filtrated with nylon mesh and washed twice by centrifugation (1000 rpm, 5 min) before being resuspended in potato dextrose broth (PDB). A single droplet of 5 μL spore suspension (5×10^5 spores/mL) was placed on a leaf of 4-week-old soil-grown *Arabidopsis* plant. Inoculated plants were kept under a transparent dome to maintain high humidity until disease lesions were recorded 2 d later.

For bacterial resistance assays, 25-d old plants were sprayed with *Pto* DC3000 *hrcC*$^-$ mutant bacteria (Yuan and He, 1996) at 5×10^8 cfu/mL, covered with a transparent dome for 1 d, and bacterial population in the leaf was determined 3 d after inoculation as described previously (Zipfel et al., 2004).

Split-Luciferase Assay

The assay was performed as previously described (Chen et al., 2008) with modifications. Briefly, *A. tumefaciens* strains containing the desired constructs were infiltrated into fully expanded leaves of 5-to-6-week-old *N. benthamiana* plants. Leaf discs were taken after 2 d, incubated with 200 μL water containing 1 mM luciferin in a 96-well plate for 10-15 min, and luminescence was captured with the GLOMAX 96 microplate luminometer or SpectraMax plate reader with LUM module. Equal expression of proteins was verified by immunoblot.

Co-Immunoprecipitation Assay

Protoplasts were isolated and transfected as previously described (Niu and Sheen, 2012), incubated overnight, and then treated with water or 1 μM flg22 for 10 min. Total protein was extracted with buffer containing 50 mM HEPES [pH 7.5], 150 mM KCl, 1 mM EDTA, 0.2% Triton X-100, 1 mM DTT, proteinase inhibitor cocktail (Roche). For anti-FLAG IP, total protein was incubated with 50 μL agarose-conjugated anti-FLAG antibody (Sigma) for 4 h, washed 6 times with extraction buffer, and the bound protein was eluted

by incubating with 60 μL of 20 μg/mL 3 × FLAG peptide (Sigma) for 1 h. The eluted protein was separated by SDS-PAGE and detected with immunoblot.

In Vitro Ubiquitination Assay

HIS- and GST-tagged recombinant proteins were expressed in *E. coli* strain BL21 and affinity-purified with glutathione-Sepharose (GE) and Ni-Sepharose (QIAGEN), respectively, following manufacturer's instructions. *In vitro* ubiquitination assays were performed as described (Zhao et al., 2012). In a basic reaction, 12.5 ng E1-HIS, 250 ng E2-HIS, 1 μg PUB25-FLAG-HIS or PUB25-HIS, and 4 μg HA-UBQ (Boston Biochem, cat. no. U-110) were incubated in 30 μL of ubiquitination reaction buffer (50 mM Tris-HCl pH 7.4, 10 mM $MgCl_2$, 5 mM ATP, 2 mM DTT) at 30°C with oscillation in a thermomixer (Eppendorf) for 2 h. For BIK1/RKS1 poly-ubiquitination, 60 ng GST-BIK1 or GST-RKS1 was added to the reaction. For heterotrimeric G proteins inhibition on PUB25 E3 ligase, 500 ng/each of XLG2CT-HIS, GST-AGB1, and GST-AGG2 were added to the reaction. For negative control, 1.5 μg BSA was added in place of the G proteins. The reaction was terminated by adding 4 × protein loading buffer and boiled at 100°C for 5 min. The sample was separated by SDS-PAGE and detected by immunoblot using anti-HA, anti-GST and anti-HIS antibodies. Poly-ubiquitination on GST-BIK1/RKS1 is indicated by ladders in the anti-GST immunoblot, whereas PUB25-HIS and PUB25-FLAG-HIS auto-ubiquitination is indicated by ladders in anti-HA and anti-HIS immunoblots, respectively.

Ubiquitination Assay in Protoplasts

Protoplasts transfected with HA-UBQ or FLAG-UBQ, PUB26-HA or PUB25-FLAG, BIK1-FLAG or BIK1-HA, and/or HA-tagged heterotrimeric G protein subunits were incubated overnight in the presence of 5 μM MG132 (Sigma). Total protein was extracted with buffer containing 50 mM HEPES [pH 7.5], 150 mM KCl, 1 mM EDTA, 0.3% Trition-X 100, 1 mM DTT, proteinase inhibitor cocktail (Roche) and incubated with agarose-conjugated anti-FLAG antibody (Sigma) in the presence of 5 μM MG132 for 4 h, washed 6 times with extraction buffer, and the bound protein was eluted with 3 × FLAG peptide (Sigma) for 1 h. The immunoprecipitates were separated by SDS-PAGE. Poly-ubiquitination on BIK1-FLAG and BIK1-HA were indicated by laddering bands in anti-HA and anti-FLAG immunoblots, respectively.

BIK1 Protein Stability in Protoplasts

To determine BIK1 protein stability, protoplasts transfected with BIK1-HA and PUB25/26-FLAG were treated with 50 μM cycloheximide (CHX [Sigma]) in the presence or absence of 1 μM flg22 for 2 h. Total protein was extracted with extraction buffer (50 mM HEPES [pH 7.5], 150 mM KCl, 1 mM EDTA, 0.3% Trition-X 100, 1 mM DTT, proteinase inhibitor cocktail [Roche]), separated in a SDS-PAGE gel and detected with anti-HA immunoblot.

Protein Degradation Assay in *N. benthamiana* Plants

A. tumefaciens strain GV3101 containing BIK1-LUC and *A. tumefaciens* strain containing WT or mutant variants of PUB25-FLAG were co-infiltrated into fully expanded leaves of *N. benthamiana* plants. Leaf discs were taken after 2 d and floated on 100 μL 100 μM CHX in a 96-well plate under dim light for 12-24 h. Then, 100 μL of 2 mM luciferin was added into each well, and luminescence was recorded with a GLOMAX 96 microplate luminometer.

LC-MS/MS Analysis

To identify BIK1-interacting proteins, BIK1-FLAG was transiently expressed in WT protoplasts, and total protein was extracted with IP buffer I (50 mM HEPES [pH 7.5], 50 mM NaCl, 10 mM EDTA, 0.2% Triton X-100, 0.1 mg/mL Dextran [Sigma], proteinase inhibitor cocktail [Roche]). Protoplasts transfected with an empty vector pUC19-35S-FLAG-RBS (Li et al., 2005) were used as negative controls. To identify PUB26 phosphosites, protoplasts expressing PUB26-FLAG were treated with 1 μM flg22 for 10 min before protein extraction. The PUB26-FLAG protein was then enriched by immunoprecipitation using anti-FLAG antibody and eluted with 75 μL 3 × FLAG peptide (Sigma) for 40-60 min according to manufacturer's instruction. The eluted proteins were separated in 10% NuPAGE gel (Invitrogen), digested with trypsin, and subject to mass spectrometric analysis. Briefly, gel slices containing the PUB26-FLAG protein were reduced with 10 mM DTT, alkylated with 55 mM iodoacetamide, and then digested overnight at 37°C with sequencing grade trypsin (Sigma, USA). The tryptic peptides were subject to LC-MS/MS analysis using an LTQ-Orbitrap elite mass spectrometer with enabled multistage activation. Proteome Discoverer software (version 1.3) (Thermo Fisher) was used for peptide identification and phosphosites assignment. The *Arabidopsis thaliana* proteome sequences (Uniprot) were used as the database and the mass tolerances were set to 10 PPM for precursor and 0.5 Da for fragment ions, and the *Arabidopsis thaliana* proteome database (Uniprot) was searched.

Generation of Antibodies

Anti-BIK1 antibodies were produced by AbMart using the following peptide: C-TGTTKSSEKRFTQK. Anti-phospho-PUB26^{T94} antibodies were produced by AbMart using a phospho-peptide: Ac-CVERIPT(p)PKQ-NH2. Antibodies that recognize non-phosphorylated peptide were depleted by incubating antisera with non-phosphorylated peptide: Ac-CVERIPTPKQ-NH2.

In Vitro Phosphorylation Assays

For phosphorylation assays, 200 ng GST-CPK28, HIS-BIK1 and HIS-BIK1^{K105E} proteins were incubated with 2 μg GST-PUB25 or GST-PUB26 in 20 μL reaction buffer (25 mM Tris-HCl [pH 7.5], 10 mM $MgCl_2$, 1 mM DTT, 100 mM ATP) for 30 min at 30°C and GST-PUB25^{T95A} and GST-PUB26^{T94A} were used as negative control. The reaction was stopped by adding SDS loading buffer. Protein phosphorylation was detected by immunoblot using anti-pT95/pT94 antibodies which specifically react with phospho-PUB25^{T95} and phospho-PUB26^{T94}.

To determine flg22-induction of CPK28 kinase activity, CPK28-FLAG was transiently expressed in *N. benthamiana* plants using *Agrobacterium*-mediated transformation, and the leaves were treated with 1 μM flg22 or water for 20 min before protein was isolated with anti-FLAG beads. Equal amounts (approximately 100 ng) of CPK28-FLAG was incubated with 2 μg GST-PUB26 protein in an *in vitro* kinase buffer, and phosphorylation of PUB26^{T94} was detected with anti-pT94/95 immunoblot.

QUANTIFICATION AND STATISTICAL ANALYSIS

Statistical significance among treatments was determined by one-way ANOVA, followed by Tukey's post hoc test at $p < 0.05$.